Eur Biophys J (2014) 43:143–155
DOI 10.1007/s00249-014-0949-x

ORIGINAL PAPER

EBSA
Biophysics in Europe

All-atom molecular dynamics study of EAK16 peptide: the effect of pH on single-chain conformation, dimerization and self-assembly behavior

Soheila Emamyari · Hossein Fazli

Received: 7 December 2013 / Revised: 17 February 2014 / Accepted: 18 February 2014 / Published online: 13 March 2014

Abstract Single-chain equilibrium conformation and dimerization of the three types of ionic EAK16 peptide are studied under three pH conditions using all-atom molecular dynamics simulations. It is found that both the single-chain conformation and the dimerization process of EAK16-IV are considerably different from those of the two other types, EAK16-I and EAK16-II. The value of pH is found to have a stronger effect on the single-chain conformation and dimerization of EAK16-IV. It is shown that in addition to the charge pattern on the peptide chains, the size of the side chains of the charged amino acids plays role in the conformation of the peptide chains and their dimerization. The results shed light on the pH-dependent self-assembly behavior of EAK16 peptide in the bulk solution, which has been reported in the literature.

Keywords Ionic complementary peptides · Self-assembly · Amphiphilic peptides · pH effect on self-assembly

Introduction

Molecular self-assembly—spontaneous aggregation of molecules or macromolecules into supramolecular structures under a variety of conditions with non-covalent interactions and without human intervention (Whitesides et al. 1991; Whitesides and Grzybowski 2002; Whitesides and Boncheva 2002)—is ubiquitous in nature. The self-assembly of proteins and peptides occurs in a number of diseases such as Alzheimer's disease, Parkinson's disease and type II diabetes (Zerovnik 2002; Soto and Saborio 2001; Ferreira and De Felice 2001; Carrell and Gooptut 1998).

Surface engineering (Zhang et al. 1999; Houseman and Mrksich 2002), drug delivery (Fernández-Carneado et al. 2004; Wang et al. 2008a), scaffolding for tissue repair (Wang et al. 2008b ; Kisiday et al. 2002; Holmes et al. 2000; Zhang et al. 1995) and fabrication of conducting nanowires (Zhang 2003; Zhang et al. 2002) are examples of applications of this phenomenon. The self-assembly of proteins and peptides may occur in the bulk or on the surface. The assembly of peptides on a surface modifies its properties and has been shown to have the potential for applications in biosensors, optical computers and solar cells (Wouters and Schubert 2004; Wei et al. 2006; Lim et al. 2006).

Because of the above-mentioned potential applications, its importance in nature and the rich basic science behind it, this phenomenon has recently attracted considerable interest from the scientists.

There is a class of peptides entitled “ionic complementary peptides” with a particular sequence of amino acids and the possibility of formation of inter- and intra-chain complementary ionic pairs. In this category, EAK16 peptide, involving EAK16-I, EAK16-II and EAK16-IV types, which have the same amino acid composition but different amino acid sequences, have been frequently used for self-assembly studies (Zhang et al. 1993; Fung et al. 2003; Jun et al. 2004; Hong et al. 2003, 2004, 2005; Wang et al. 2008a; Luo et al. 2008; Yang et al. 2007a, b). The first discovered peptide of this family is EAK16-II, which is a small part of Zuotin protein. Zhang and co-workers were

S. Emamyari · H. Fazli (✉)
Department of Physics, Institute for Advanced Studies in Basic Sciences (IASBS), 45137-66731 Zanjan, Iran
e-mail: fazli@iasbs.ac.ir

H. Fazli
Department of Biological Sciences, Institute for Advanced Studies in Basic Sciences (IASBS), 45137-66731 Zanjan, Iran

the first group who reported the existence of Zuotin protein in 1992 (Zhang et al. 1992). Since then, many groups have studied the self-assembly behavior of EAK16 peptide (Jun et al. 2004; Hong et al. 2003, 2004, 2005; Wang et al. 2008a; Luo et al. 2008; Yan et al. 2008).

By study of the self-assembly behavior of EAK16 peptide in the bulk solution, it has been shown that at neutral pH, EAK16-I and EAK16-II peptides assemble into fibrillar structures, while EAK16-IV forms globular assemblies (Jun et al. 2004). Also, study of the self-assembly behaviors of EAK16-II and EAK16-IV peptides at different pH conditions has shown that EAK16-IV has a pH-dependent behavior unlike EAK16-II, whose self-assembly behavior is less sensitive to the pH value (Hong et al. 2003). Adsorption of EAK16-II peptide chains to a hydrophobic surface under different pH conditions has also been studied using all-atom molecular dynamics simulation, and it has been shown that inter-chain electrostatic interactions affect the adsorption rate (Sheng et al. 2010). In a recent work, we have studied pH-dependent self-assembly behavior of the three types of EAK16 peptide in the presence of a hydrophobic surface using a coarse-grained model and molecular dynamics simulation (Emamyari and Fazli 2014). We have shown that EAK16-I and EAK16-II peptides assemble into ribbon-like structures on the hydrophobic surface, regardless of the pH value. EAK16-IV peptide however, assembles into ribbon-like structures at low and high pH ranges and forms disc-shaped assemblies at the isoelectric point, pH = 7, on the hydrophobic surface.

Self-assembly behavior of macromolecules depends on numerous parameters such as inter- and intra-molecular interactions, solvent properties, architecture of the molecules, and presence or absence of objects that accelerate or prevent the aggregation and the ordering processes. For example, presence of an interacting surface causes the self-assembly behavior of macromolecules to be considerably different from that in the bulk solution. Understanding the detailed mechanism of the self-assembly of simple macromolecules such as short peptides is very useful for shedding light on very complex versions of this phenomenon that happen in nature and living systems. Especially, describing the roles of relevant parameters in detail is of great importance.

The nucleation step of the self-assembly process in the solution of self-assembling materials starts to happen from the single-molecule level. In addition, the molecules of the self-assembling material are the main building blocks in the growth stage of the assemblies. Accordingly, study of the behavior of single molecules and the dimerization process in the atomic scale using molecular dynamics simulations is important for better understanding the details of the self-assembly phenomenon. Although study of a many-molecule system in the atomic scale can generate very useful information, it is too time consuming with ordinary computational devices. Study of single- and double-molecule systems in atomic scale, which is possible in a reasonable time, in combination with physical interpretation and generalization of the results to many-molecule systems seems to be a possible and feasible way.

In this article, we present the results of all-atom molecular dynamics study of the single-chain conformation and the dimerization behavior of the three types of EAK16 peptide under three pH conditions. Our results show that both the single-chain conformation and the dimerization process of EAK16-IV are considerably different from those of the two other types. The value of pH is found to have a stronger effect on the single-chain conformation and the dimerization of EAK16-IV. Also, it is found that in addition to the charge pattern on the peptide chains, the size of the side chains of amino acids plays a role in the conformation of the peptide chains. Using the simulation results, we describe different pH-dependent behaviors of single- and double-chain systems of the three types of EAK16 peptide and present a description of pH-dependent self-assembly behavior of these peptides in the bulk solution.

Molecular structure of the three types of EAK16 peptide

All three types of EAK16 peptide are composed of alternating hydrophobic (alanine) and ionic (lysine and glutamic acid) amino acids. They have 16 amino acids and the sequences of EAK16-I, EAK16-II and EAK16-IV are $(AEAK)_4$, $(AEAEAKAK)_2$ and AEAEAEAEAKAKAKAK, respectively (see Fig. 1). At pH = 7, the hydrophilic monomers 'E' and 'K' carry net negative and positive electric charges, respectively. The hydrophobic

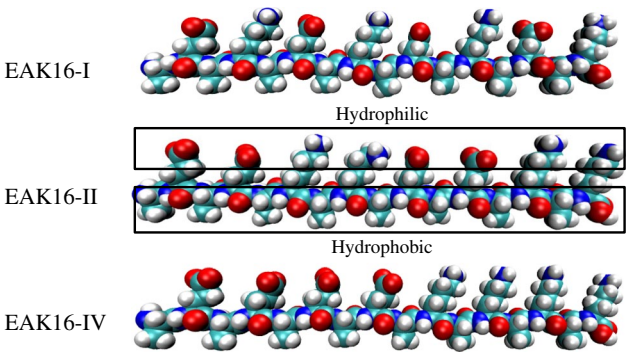

Fig. 1 Schematic three-dimensional molecular model of EAK16-I, EAK16-II and EAK16-IV. Carbon, oxygen, nitrogen and hydrogen atoms are shown as *cyan*, *red*, *blue* and *white spheres*, respectively. EAK16 peptides are amphiphilic and contain hydrophilic and hydrophobic sides as demonstrated in the molecular structure of EAK16-II

monomer 'A' carries no net electric charge. Accordingly, the charge distributions of EAK16-I, EAK16-II and EAK16-IV at the isoelectric point, pH = 7, are: $-+-+-+-+$, $--++--++$ and $----++++$, respectively. These peptides are amphiphilic. The side of each peptide chain to which the side chains of 'E' and 'K' monomers are oriented is hydrophilic, and the opposite side is hydrophobic (see Fig. 1).

pK_a values of the side chains of lysine and glutamic acid are 10.53 and 4.3, respectively. This means that at pH values lower than 4.3 (called a low pH condition here), all glutamic acids neutralize and lysines remain charged, and EAK16 peptide chains carry a net positive charge. On the other hand, at pH values greater than 10.53 (high pH condition), all lysines neutralize and glutamic acids remain charged, and EAK16 chains carry an absolute negative charge.

It should be noted that the side chains of the ionic amino acids, lysine and glutamic acid, are of different sizes (lysine has a longer side chain relative to glutamic acid). Arising from this difference between the mentioned amino acids, the single-chain conformation of an EAK16 peptide of each type in a low pH condition (positively charged lysines and neutral glutamic acids) may be different from that in a high pH condition (negatively charged glutamic acids and neutral lysines). We will discuss this point in "Results" and "Conclusion".

Simulation details

All of the simulations are carried out with GROMACS package, version 4-0-7 (van der Spoel et al. 2005a, b; Hess et al. 2008) in NPT ensemble. A dodecahedron simulation box with the edge length $l = 6\ nm$ is used. The volume of the simulation box in single-chain simulations is 152 nm^3. The box edge and box volume in double-chain simulations are 10 nm and 707 nm^3, respectively. The simulation box is filled with about 5,000 (23,000) Single-Point Charge (SPC) water molecules in single- (double-) chain simulations (Berendsen et al. 1981). Lincs method is used to constrain all of the bond lengths to their equilibrium values (Hess et al. 1997), and the Settle algorithm is used to constrain water molecules (Miyamoto and Kollman 1992). Electrostatic interactions are calculated using the particle-mesh Ewald (PME) method with a cutoff distance of 1.0 nm (Darden et al. 1993; Essmann et al. 1995). The peptide and water molecules are coupled separately to a temperature bath of constant temperature, $T = 300°K$, with a coupling constant of 0.1 ps using the Berendsen algorithm. The pressure of the system is also kept fixed in the same way at 1 bar with a coupling constant of 1 ps (Berendsen et al. 1984). The periodic boundary condition is used in all of the simulations. A cutoff length of $\lambda_c = 1$ nm is used for calculation of Lennard-Jones interactions. The neighbor list is updated every ten steps, with a neighbor list cutoff distance of 1 nm.

Before running the simulation of the system for each given set of the parameters, we subject it to a 3,000-step steepest descent optimization to relax unfavorable contacts, followed by a 20-ps MD equilibration simulation with positional restraints on the peptide atoms using a leap-frog algorithm in an NPT ensemble (van Gunsteren and Berendsen 1988). The force constant on the peptide atoms in each direction (x, y and z) is 1,000 kJ/ (mol nm^2). After equilibration, full simulations are performed using an OPLS.AA all atom force field with a time step of 2 fs (Jorgensen and Tirado-Rives 1988). The VMD package is also used to visualize the conformation of the peptide chains (Humphrey et al. 1996).

In an experimental study of the self-assembly phenomenon of EAK16 peptide, the N(C)-terminus of the peptide chains is protected by acetyl(amino) group to avoid end-to-end electrostatic attraction between the peptides (Jun et al. 2004). For the same purpose and regarding our available force fields, we use NH_2 and COOH groups instead of NH_3^+ and COO^- in the N- and C-terminal of the peptides to study them with no electric charges in their terminals. To make the system electrically neutral in low (high) pH condition, four Cl^- (Na^+) ions are added to the solution. In the beginning of each simulation, each peptide chain is in its extended conformation among water molecules. We produce the initial conformation of the peptide chains using the HyperChem software (HyperChem™, Hypercube, Inc., USA). We consider the time it takes the total energy of the system to reach a stable value as the system equilibration time. It is found that this time is at most 10 ns. The values of desired quantities are averaged over time after equilibration of the system. To probe the time evolution of the conformation of a peptide chain, we calculate its radius of gyration in the course of the simulation. We also calculate time-averaged separation between the amino acids of each peptide chain after equilibration of the system. The separation between a pair of amino acids along a peptide chain is defined as the separation between their center of mass. Also, we calculate the average number of intra- and inter-chain hydrogen bonds in the simulations. In addition, snapshots of the system along the simulations are used for probing the conformational evolution of the peptide chains and for comparison with the quantitative results.

Results

The first step for understanding the collective behavior of the peptide chains in the solution is the study of the

equilibrium behavior of a single peptide chain. Consider the situation that the peptide concentration in the solution is not so high and the peptide chains do not overlap with each other before the self-assembly process (the peptide concentration is below the overlap concentration). In this situation, the individual peptide chains have enough time to find their equilibrium conformation dictated by intra-chain and chain-solvent interactions before interacting with the other peptide chains. Hence, with the aim of study of a peptide solution below the overlap concentration, we first study a single-chain system for the three types of EAK16 peptide at three pH conditions and describe the equilibrium conformation of the chain. Then, to study the dimerization process of the peptide chains and the effect of inter-chain interactions on their conformation, we perform simulations of double-chain systems with the same method. Combination of the results of single- and double-chain simulations gives insight into the self-assembly phenomenon of the peptide chains in a many-peptide system.

Results of single-chain simulations

The density plot of the time-averaged separations between the amino acids of each peptide chain in three pH conditions are shown in Fig. 2. The separations between the amino acids are averaged over time from $t = 150$ ns to

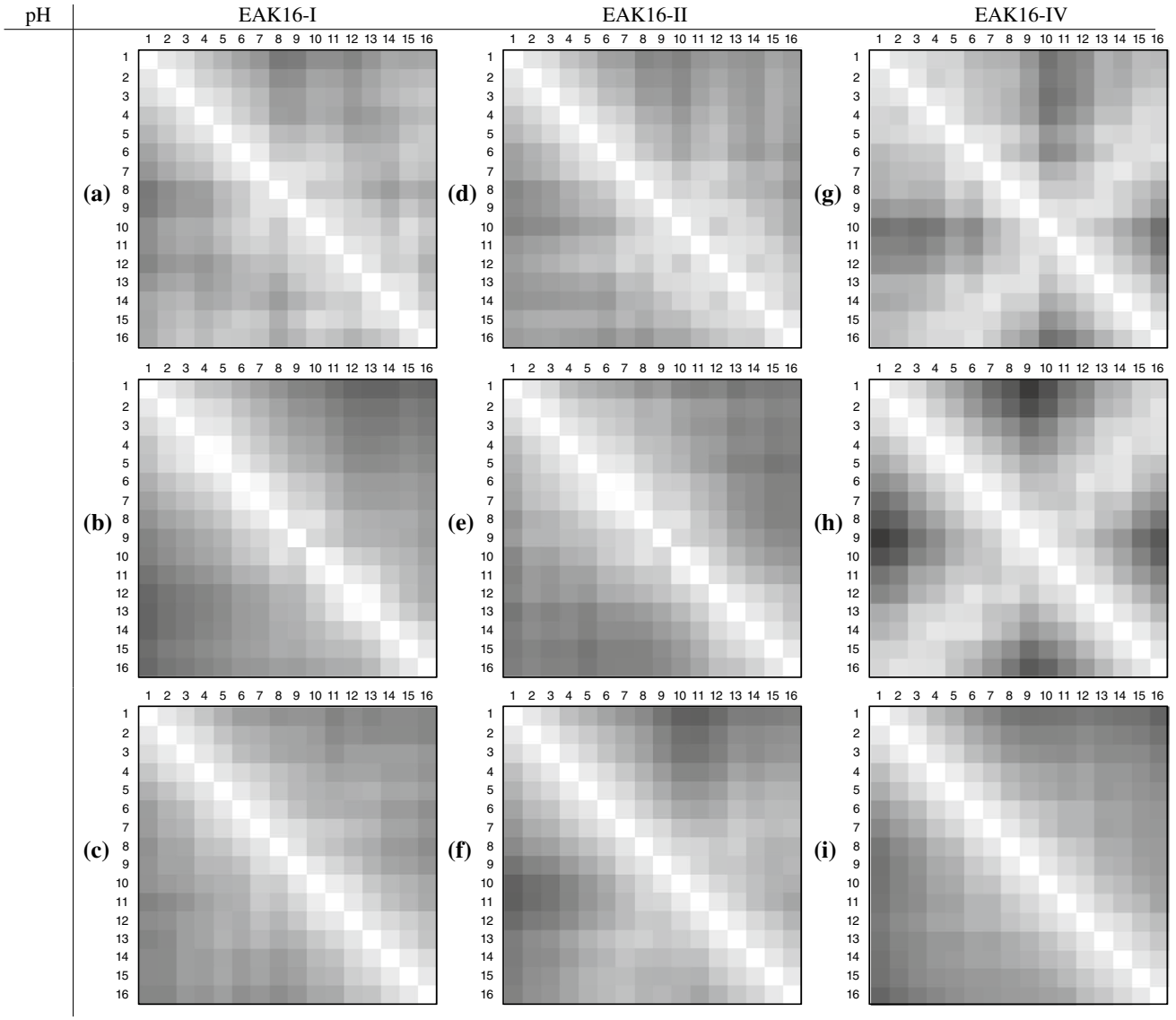

Fig. 2 Density plot of the time-averaged separations between pairs of amino acids of peptide chains for EAK16-I at pH < 4.3 (**a**), neutral pH (**b**) and pH > 10.53 (**c**), EAK16-II at pH < 4.3 (**d**), neutral pH (**e**) and pH > 10.53, (**f**) and EAK16-IV at pH < 4.3 (**g**), neutral pH (**h**) and pH > 10.53 (**i**). The averages are calculated over time from $t = 150$ ns to $t = 250$ ns. *Darkness of the squares*, which corresponds to the separation between amino acids, ranges from 0 to 2.32 σ

$t = 250$ ns. It has been checked that averaging over other time intervals (for example, from $t = 200$ ns to $t = 250$ ns) gives similar results. In each panel of this figure, the gray scale of square in row i and column j reflects the time-averaged separation between amino acids i and j of the peptide chain. The darker the square in row i and column j, the larger the time-averaged separation between amino acids i and j of the corresponding peptide chain. It should be noted that a large and positive gradient of the darkness of squares in the first row of each panel shows that the corresponding chain has dominantly extended conformation (see, for example, Fig. 2b). A region containing light squares perpendicular to the main diagonal of a panel shows that the corresponding chain has dominantly hair-pin shaped conformation (see Fig. 2h, for example). A panel without a light region perpendicular to the main diagonal and with no large gradient of the darkness of the squares of the rows shows that the corresponding peptide chain dominantly has a loosely curved conformation (for example, see Fig. 2d). The reason for this claim is described in Fig. 3. For a peptide chain with a circularly curved conformation, the differences between monomer-monomer separations are smaller than those for a peptide with extended conformation (compare the differences between the sizes of the vectors shown in Fig. 3b with those in Fig. 3c). A small gradient of the darkness of squares in the rows of Fig. 2d and absence of a light region of squares perpendicular to the main diagonal in this panel show that the dominant conformation of the corresponding peptide chain is similar to that in Fig. 3a.

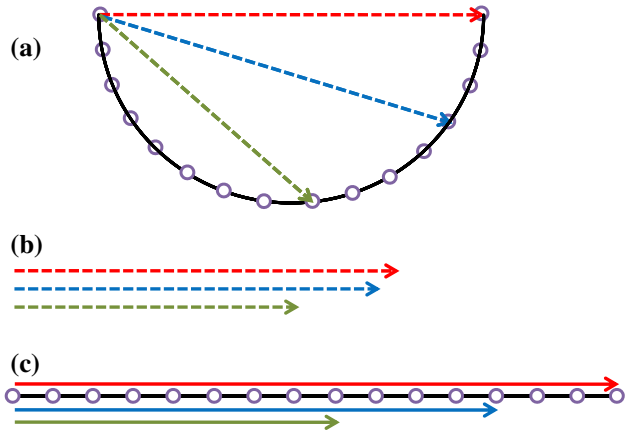

Fig. 3 Spatial distance of the 9th (*green*), 13th (*blue*) and 16th (*red*) monomer of a polymer containing 16 monomers from its first monomer when the polymer is circularly curved (**a**). The separation vectors are also shown for comparison (**b**). Separations between the monomers for the same polymer when it has extended conformation (**c**). As is shown, the differences between the separations are smaller when the peptide chain has a curved conformation. This is the reason for the smaller gradient of the darkness of squares in some panels of Figs. 2, 8 and 11, which correspond to the loosely curved conformation of the peptide chains

Radius of gyration of the three types of EAK16 peptide versus time obtained from single-chain simulations at three pH conditions are shown in Fig. 4. It can be seen that at low pH conditions, the radius of gyration of all three peptides decreases as time lapses and takes small values showing that all three types tend to have small spatial expansion in this pH condition. This arises from intra-chain interactions. One should note that in this pH condition, glutamic acids are neutral and lysines are charged. By taking a curved or hair-pin shaped conformation, a peptide chain keeps its hydrophobic side chains from being exposed to water and increases the separation between the charged heads of the side chains of lysines, simultaneously. In the case of EAK16-IV, lysines are closer to each other along the chain relative to the two other types and stronger electrostatic repulsion between their side chains forces this peptide to take a greatly curved conformation. The signature of the folded conformation of the EAK16-IV chain in low pH conditions can be obviously seen in Fig. 2g. One should note that the large fluctuations in the value of the gyration radius, as can be seen in Fig. 4, are not related to the equilibration of the system. Large fluctuation shows that intra-chain interactions are not strong enough relative

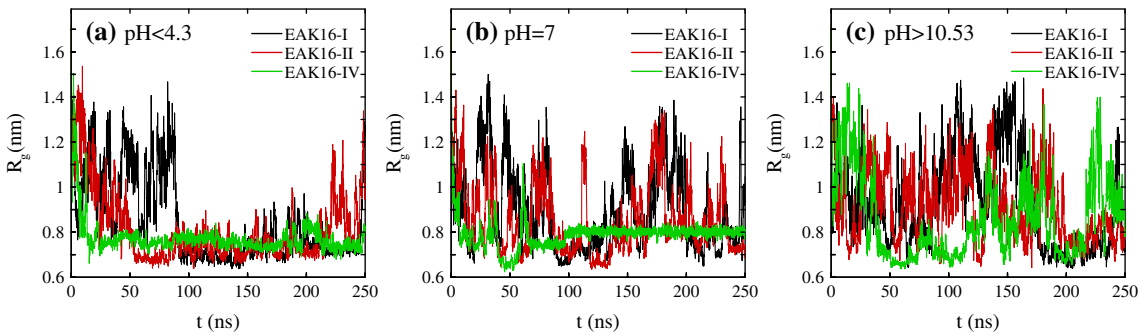

Fig. 4 Radius of gyration of the three types of EAK16 peptide at pH < 4.3 (**a**), neutral pH (**b**) and pH > 10.53 (**c**) versus time obtained from single-chain simulations of each type

to the thermal energy to fold the corresponding chain and the chain size fluctuates as a flexible polymer in a good solvent. In this pH condition, the number of intra-chain hydrogen bonds averaged over the simulation time for EAK16 chains of types I, II and IV is 3.5 ± 2.3, 4.4 ± 2.1 and 5.0 ± 1.6, respectively. Non-integer values of these numbers and their standard deviations come from averaging over the simulation time.

As can be seen in Fig. 4b, at the isoelectric point, pH = 7, only EAK16-IV peptide has a small spatial expansion, and its radius of gyration versus time has small fluctuations. It is quite different from the behaviors of the two other types, EAK16-I and EAK16-II, which have larger spatial expansions and larger conformational fluctuations. In fact, at this pH condition, the thermal fluctuations are capable of changing the conformation of the peptides EAK16-I and EAK16-II because of their weak intra-chain electrostatic attraction. In the case of EAK16-IV, because of the strong electrostatic attraction between the side chains of oppositely charged monomers, lysines and glutamic acids, the chain dominantly takes a hairpin-shaped conformation, and the hydrophobic side chains of alanines have to be exposed to water (see Fig. 5h). Hence, in neutral pH, it is expected that the folded EAK16-IV chains attract each other hydrophobically and form globular structures, as has been observed experimentally (Jun et al. 2004). In this pH condition, the number of intra-chain hydrogen bonds averaged over the simulation time for EAK16 chains of types I, II and IV are 5.1 ± 2.3, 5.3 ± 2.1 and 7.4 ± 2.2, respectively. In this pH condition, in addition to strong electrostatic attraction between oppositely charged halves of the EAK16-IV chain, intra-chain hydrogen bonds help the chain to keep its hair-pin-shaped conformation.

Under high pH conditions, pH > 10.53, as can be seen in Fig. 4c, the peptide chains of all three types have a large gyration radius with large fluctuations. Negatively charged glutamic acids are closer to each other in EAK16-IV, and there is stronger electrostatic repulsion between the similarly charged heads of their side chains relative to EAK16 peptides of the two other types. The same scenario for lysines is in low pH conditions. However, as can be seen in Fig. 4c, it does not cause EAK16-IV peptide to take a very curved conformation relative to the peptides of the two other types in this pH condition. One should note that such differences between the cases of low and high pH conditions arise from the difference between the sizes of the side chains of lysine and glutamic acid. As mentioned in Sect. II, the side chain of lysine is longer than that of glutamic acid, and the heads of the side chains are charged in both of the amino acids. One can imagine that longer side chains with similarly charged heads have a stronger effect on bending of the peptide backbone relative to the shorter ones. For the extreme case that the length of the side chain is zero (the charges are distributed on the backbone of the chain), it is known from the properties of polyelectrolytes that the repulsion between the charges causes the chain to take an extended conformation. In this pH condition, the average number of intra-chain hydrogen bonds for EAK16 chains of types I, II and IV are 3.3 ± 1.9, 3.9 ± 1.9 and 4.0 ± 2.2, respectively.

Sample snapshots of the peptide chains under three pH conditions are shown in Fig. 5. In this figure, all of the atoms of each peptide are shown in the same color, and the backbones of the peptide chains are shown as a ribbon for clarity. Combination of the density plots shown in Fig. 2 and the sample snapshots shown in Fig. 5 gives insight into the dominant conformations of the peptide chains in different pH conditions.

Results of double-chain simulations

Considering the results of single-chain simulations that reveal the equilibrium conformation of single peptide chains, we perform double-chain simulations to study the dimerization process of the peptides at three pH ranges. To avoid time-consuming simulations of the diffusion processes of the peptide chains toward each other, we start these simulations from initial configurations in which the peptides are close to each other and the system has the lowest interaction energy (statistically the most likely conformation of the peptide chains relative to each other). For example, single-chain simulations of EAK16-I at all pH ranges showed that it dominantly takes an extended conformation. Hence, in double-chain simulations of EAK16-I, we consider two extended chains close to each other in parallel and antiparallel states. These chains are slightly shifted relative to each other to avoid their similarly charged amino acids from being in front of each other (see Fig. 6). In the case of EAK16-IV chains at low and high pH conditions, similarly charged parts of the chains are oriented in opposite directions, as shown in Fig. 7. In fact, in this case the only attractive interaction between the chains is the hydrophobic interaction. Because of very similar results of the simulations of EAK16-I and EAK16-II double-chain systems, only the results of the simulations of the EAK16-I double-chain system are shown here.

In the case of EAK16-IV peptide under neutral pH conditions, the intra-chain electrostatic interaction is strong enough that it forces the hydrophobic side chains of the chain to be exposed to water. It is expected that folded hair-pin-shaped EAK16-IV chains with exposed hydrophobic side chains attract each other in a many-peptide system and form globular assemblies. Formation of globular assemblies by the EAK16-IV peptide around neutral pH has been also observed in coarse-grained simulation of many-peptide systems (Emamyari and Fazli 2014).

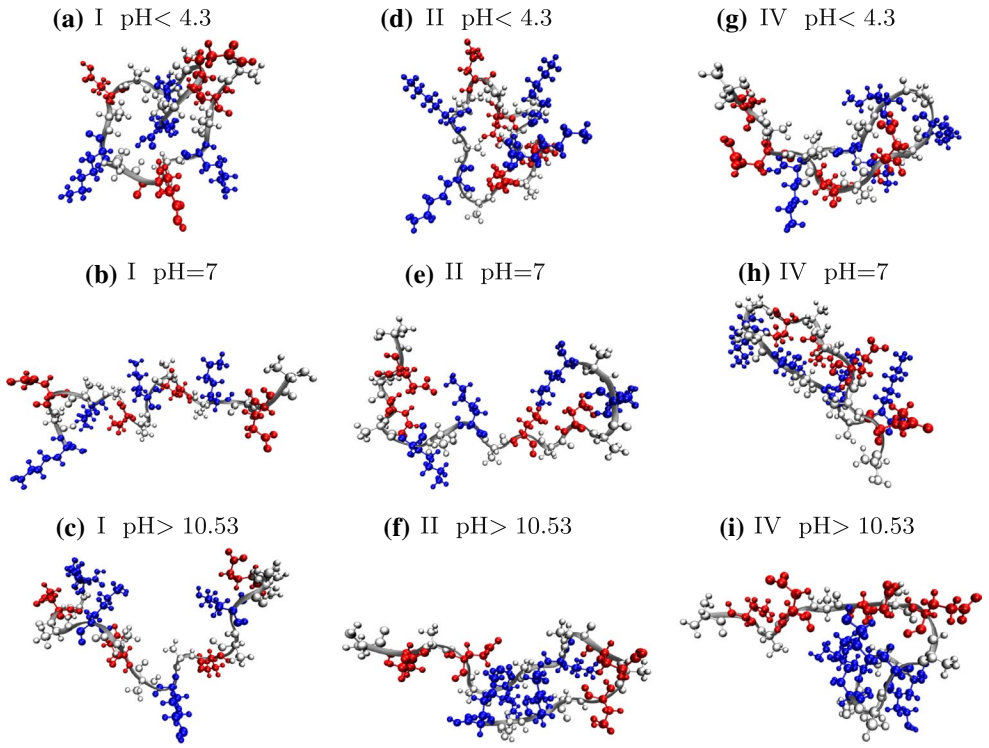

Fig. 5 Sample snapshots of the peptide chains taken from single-chain simulations of EAK16-I at pH < 4.3 (**a**), neutral pH (**b**) and pH > 10.53 (**c**), EAK16-II at pH < 4.3 (**d**), neutral pH (**e**) and pH > 10.53 (**f**), and EAK16-IV at pH < 4.3 (**g**), neutral pH (h) and pH > 10.53 (**i**)

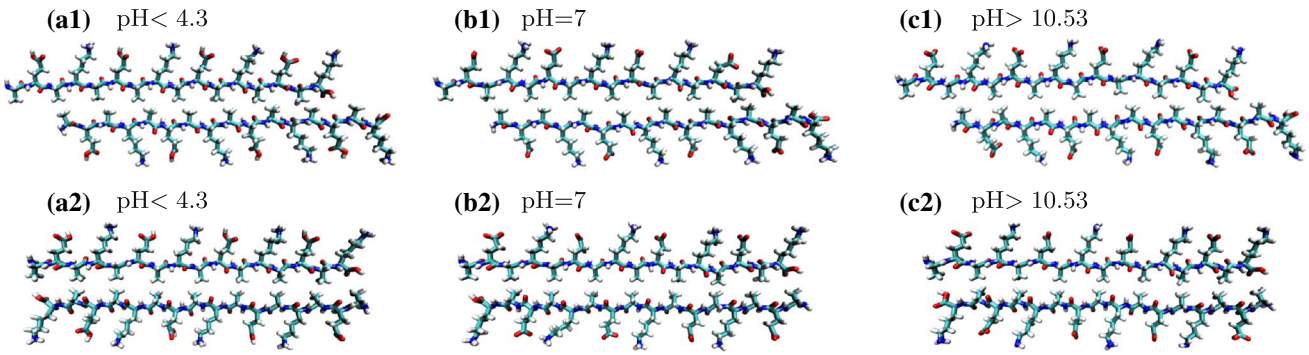

Fig. 6 Initial configurations (parallel and antiparallel) of the two EAK16-I peptide chains in their simulations in low (*a1*, *a2*), neutral (*b1*, *b2*) and high (*c1*, *c2*) pH conditions. In antiparallel configurations, the chains are slightly shifted relative to each other to avoid the similarly charged amino acids from being in front of each other. Carbon, oxygen, nitrogen and hydrogen atoms are shown in *cyan*, *red*, *blue* and *white*, respectively. The numbers of inter-chain hydrogen bonds in the corresponding simulations are obtained as: 3.1 ± 1.2 (*a1*), 8.2 ± 3.0 (*a2*), 4.7 ± 1.7 (*b1*), 4.5 ± 1.8 (*b2*), 5.8 ± 2.4 (*c1*) and 4.5 ± 1.7 (*c2*)

In Fig. 8, the density plots of the time-averaged separations between amino acids of a chain (also averaged over two peptide chains) obtained from double-chain simulations of EAK16-I in three pH conditions and for parallel and antiparallel initial configurations of Fig. 6 are shown. As can be seen in this figure, EAK16-I chains in low and high pH conditions have more extended conformation relative to the neutral pH condition. At pH = 7, the two chains take a curved conformation after dimerization. Having smaller spatial expansion in this pH condition is expected for EAK16-I chains. It is known from properties of polyampholytes that they have small radius of gyration at the isoelectric point relative to basic and acidic pH conditions (Dubrynin et al. 2004). Radii of gyration of the two peptide chains versus time obtained from six double-chain simulations of EAK16-I (parallel and antiparallel initial

configurations under three pH conditions) are shown in Fig. 9. As can be seen, at pH = 7, when the chains are antiparallel, the dimer of the chains has the smallest gyration radius. Sample snapshots of the chains for the six above-mentioned simulations are shown in Fig. 10.

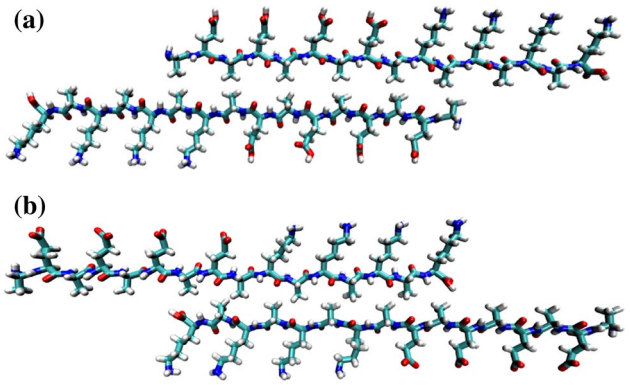

Fig. 7 Initial configurations of the two EAK16-IV peptide chains in double-chain simulations in low (**a**) and high (**b**) pH conditions. In these configurations, similarly charged blocks of the chains are oriented in opposite directions to minimize the electrostatic energy of the system. Carbon, oxygen, nitrogen and hydrogen atoms are shown in *cyan*, *red*, *blue* and *white*, respectively. The numbers of inter-chain hydrogen bonds in the corresponding simulations are obtained as: 8.8 ± 3.5 (**a**), 7.6 ± 2.0 (**b**)

Density plots of the time-averaged separations between the amino acids of each chain (averaged over the chains) obtained from EAK16-IV double-chain simulations in low and high pH conditions are shown in Fig. 11. From the larger gradient of the darkness of the squares in the rows of the panel (b) relative to that of panel (a), it can be concluded that at high pH conditions the peptide chains have a more extended conformation. In low pH conditions, although the chains do not have a hair-pin-shaped conformation [there is no light region of squares perpendicular to the main diagonal of panel (a)], a small gradient of the darkness of squares in rows of this panel shows that the chains have a loosely curved conformation. Radius of gyration versus time for the two EAK16-IV chains is shown in Fig. 12. Smaller spatial expansion of the chains in low pH conditions relative to high pH conditions can be also seen in this figure. Sample snapshots of the dimer of EAK16-IV peptide in low and high pH conditions are shown in Fig. 13. The average number of inter-chain hydrogen bonds in simulations of double-chain systems with initial configurations shown in Figs. 6 and 7 are presented in the captions of these figures.

Discussion

Experimental studies of the self-assembly of EAK16 peptide in bulk solution have shown that EAK16-IV assembles

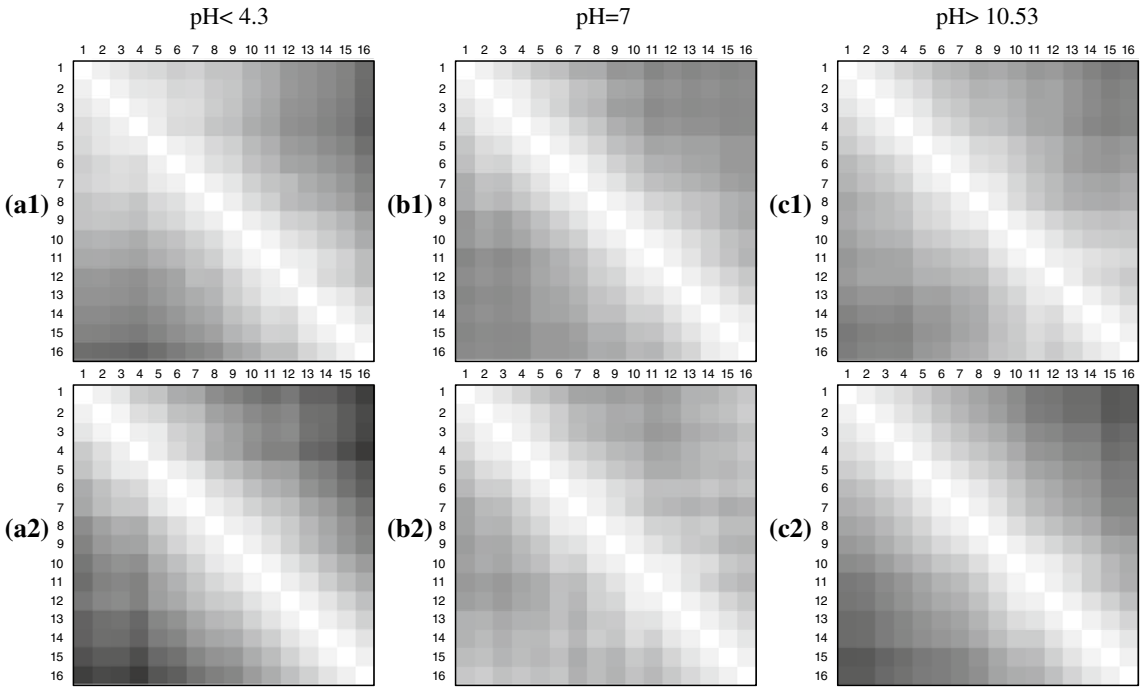

Fig. 8 Density plots of the time-averaged separations between amino acids of the two EAK16-I peptide chains in simulations of the double-chain systems in low pH condition, pH < 4.3 (*a1*, *a2*), at pH = 7 (*b1*, *b2*) and in high pH condition, pH > 10.53 (*c1*, *c2*). The separations between the amino acids are averaged over time from $t = 10$ ns to $t = 50$ ns. *Darkness of the squares*, which corresponds to the separation between amino acids, ranges from 0 to 3.05 σ

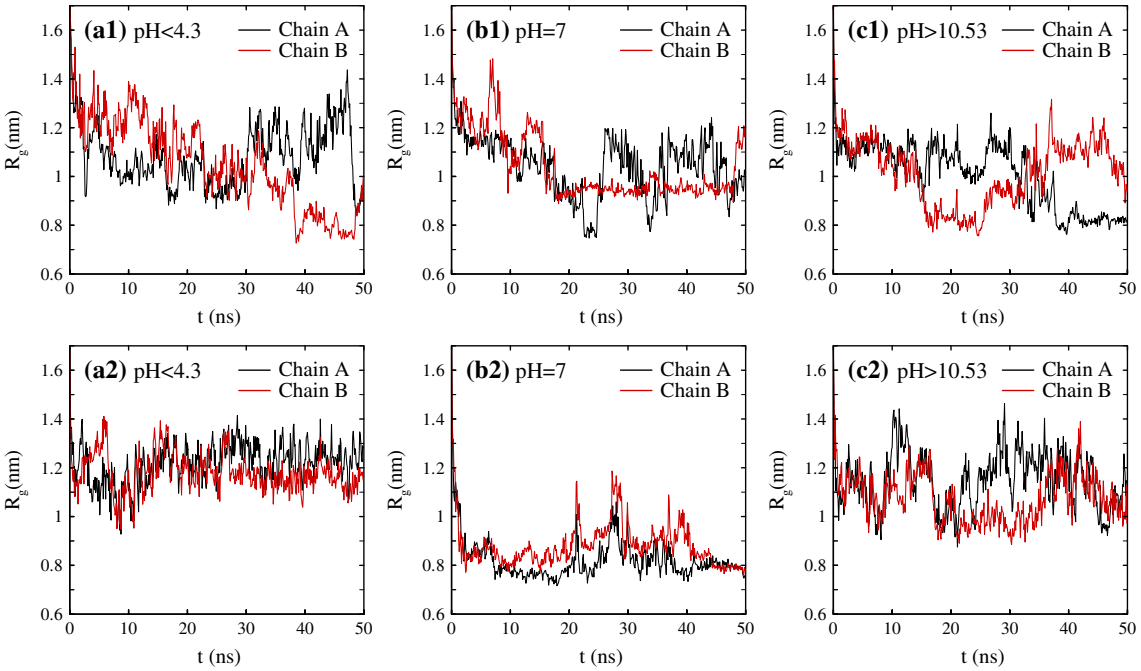

Fig. 9 Radius of gyration for the two EAK16-I peptide chains obtained from simulations of double-chain systems in low pH condition, pH < 4.3 (*a1*, *a2*), at pH = 7 (*b1*, *b2*) and in high pH condition, pH > 10.53 (*c1*, *c2*)

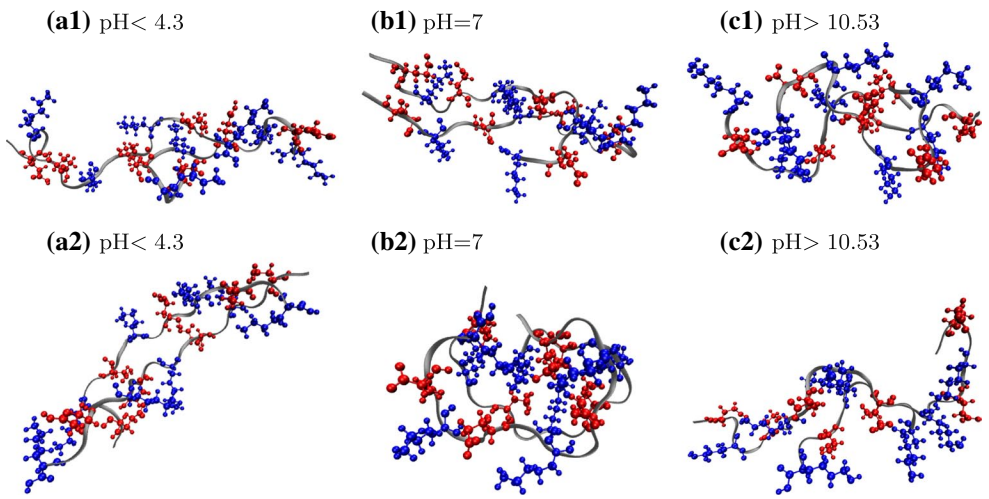

Fig. 10 Snapshots of two EAK16-I peptide chains from simulations of a double-chain systems in low pH condition, pH < 4.3 (*a1*, *a2*), at pH = 7 (*b1*, *b2*) and in high pH condition, pH > 10.53 (*c1*, *c2*)

into globular structures under neutral pH conditions and forms fibrillar assemblies under low and high pH conditions. The two other types, EAK16-I and EAK16-II, however, assemble into fibrillar structures regardless of the pH value. Our study shows that a signature of the difference between the self-assembly behavior of EAK16-IV and those of the two other types of EAK16 can be seen in single- and double-chain levels. As is shown in Figs. 2 and 4, single-molecule simulations of the three types of EAK16 peptide in three pH conditions show that only EAK16-IV peptide has a folded conformation under low and neutral pH conditions. Such a folded conformation at the level of a single molecule has potential for formation of globular assemblies. A closer study of the EAK16-IV molecule under low and neutral pH conditions shows that only in neutral pH are its hydrophobic side chains exposed to water, which provides the possibility of formation of globular assemblies driven by the hydrophobic interaction.

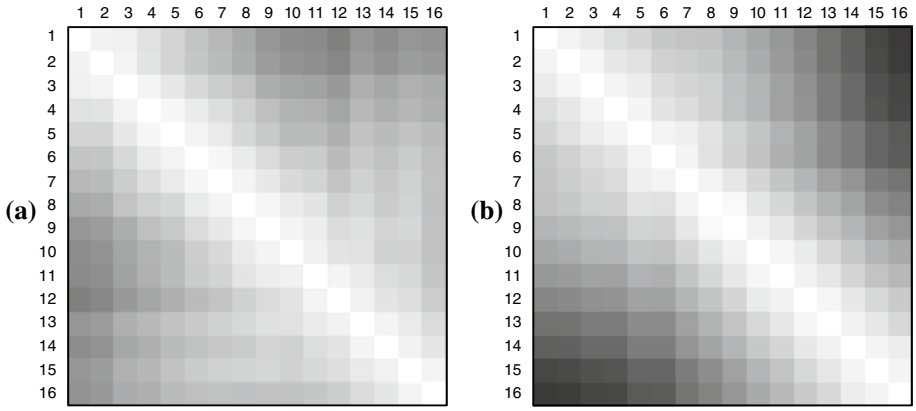

Fig. 11 Density plot of the time-averaged separations between amino acids of the two EAK16-IV peptide chains in simulations of double-chain systems in low (**a**) and high (**b**) pH conditions (averaged over the two chains). Averages over time are calculated from $t = 10$ ns to $t = 50$ ns. *Darkness of the squares*, which corresponds to the separation between amino acids, ranges from 0 to 3.49 σ

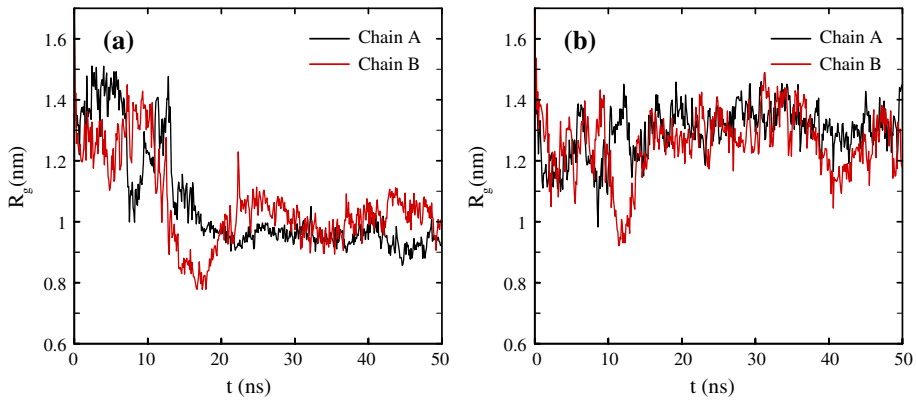

Fig. 12 Radius of gyration for the two EAK16-IV peptide chains in simulations of double-chain systems in low (**a**) and high (**b**) pH conditions

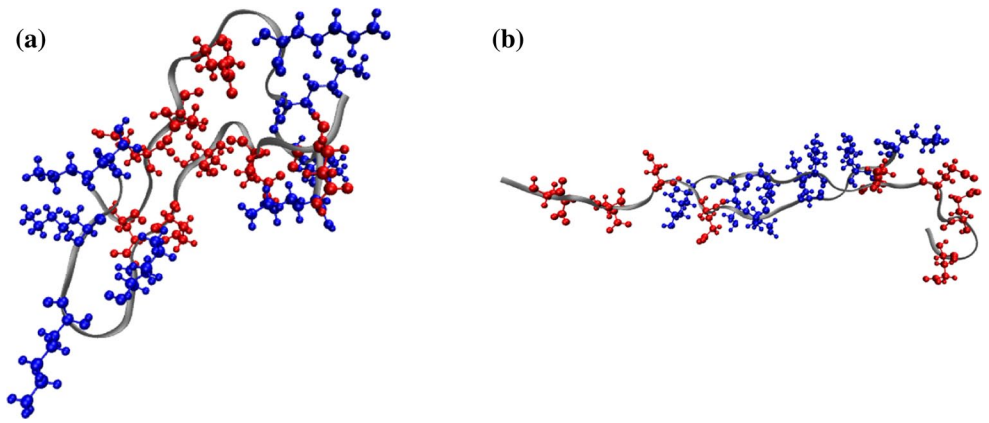

Fig. 13 Snapshots of two EAK16-IV peptide chains from simulations of double-chain systems in low (**a**) and high (**b**) pH conditions

Unlike the neutral pH condition under which a strong intra-chain electrostatic attraction keeps the chain folded with the hydrophobic side chains exposed to water, in low pH conditions there is no such strong intra-chain electrostatic attraction, and the peptide chain tends to have an extended conformation in a many-chain system. It can be seen in Figs. 11 and 12 that the folded conformation of EAK16-IV at the single-molecule level and in low pH condition does not persist at the dimer level. Accordingly, the folded conformation of the single chain in low pH condition does not result in the formation of a globular assembly in a many-chain system.

EAK16 is an amphiphilic and ionically complementary peptide, and the interplay between hydrophobic and electrostatic interactions has a determining role in its equilibrium conformation, dimerization process and the self-assembly behavior. By tuning the strength of the electrostatic interactions or the charge distribution on EAK16 peptide chains,

one can affect their conformation, dimerization and self-assembly behavior. The pH value of the solution affects the electrostatic interaction between the amino acids by affecting the net charge on their side chains. Depending on the pH value and other related factors such as the ionic strength of the solution, electrostatic interactions may be strong or weak relative to the thermal energy, k_BT. For example, in the case of EAK16-IV in neutral pH conditions, intra-chain electrostatic attraction dominates over thermal fluctuations, and the folded molecules with their hydrophobic side chains exposed to water tend to form globular assemblies. In the case of EAK16-IV in low pH conditions, however, the interaction that folds the single molecule is not strong enough relative to the thermal and hydrophobic interaction to keep the chains folded at higher levels of the self-assembly process, and in the course of the dimerization process the chains take an extended conformation.

Concerning our simulations of the dimerization process of EAK16 peptides, one should note that the simulations have been started from initial configurations that statistically have a considerably high chance of happening. In reality, two peptide chains may have quite different configurations when they see each other in the solution and start the dimerization process. This also causes the chains to experience different trajectories and probably many local minima arising from the combination of hydrophobic and electrostatic interactions in the course of the dimerization process. Hence, the initial configurations in our simulations at most can be considered as ones of high probability, and the other initial configurations also have a chance to happen.

Conclusion

In conclusion, the effect of the pH value on the single-chain equilibrium conformation and the dimerization process of the three types of EAK16 peptide have been studied using all-atom molecular dynamics simulations, and their self-assembly behavior has been discussed accordingly. It has been shown that both the single-chain conformation and the dimerization behavior of EAK16-IV are noticeably different from those of the two other types, and the pH value has a stronger effect on EAK16-IV. It has been found that in addition to the charge pattern on the peptide chains, the difference between the sizes of the side chains of ionic amino acids, lysine and glutamic acid, plays an important role in the single-chain conformation and dimerization of the peptide chains. The longer side chain of lysine relative to glutamic acid causes the single-chain conformation of the EAK16-IV peptide in low and high pH conditions to be different, despite the same sequence of similarly charged amino acids on the peptide chain in both pH conditions.

Also, it has been found that the electrostatic attraction between oppositely charged blocks of EAK16-IV peptide at the isoelectric point, pH = 7, causes this peptide to take a folded-hair-pin-shaped conformation and its hydrophobic side chains to be exposed to water. From this observation, the globular assembly of this peptide at pH = 7, which has been observed in the experiment, can be described. In fact, in this pH condition, the strong intra-chain electrostatic attraction causes the hydrophobic interaction to be the dominant inter-chain interaction that forces the peptide chains to form globular assemblies. In cases of the two other types of EAK16 peptide, the intra-chain electrostatic attraction is not strong enough relative to the thermal fluctuations to fold the peptide chains and expose their hydrophobic side chains to water. It has been observed experimentally that these two peptides assemble into fibrillar structures at all pH conditions.

The other point that can be concluded here is the effect of the length of the blocks of similarly charged monomers on the self-assembly behavior of an ionic complementary peptide. In the peptides with small blocks of charged monomers, intra-chain electrostatic interactions are not capable of overcoming the entropic barrier against the folding of the chains. Such peptide chains have a tendency toward forming fibrillar assemblies. The peptides containing larger blocks of similarly charged monomers however, tend to form globular assemblies in the bulk. Also, it can be concluded from our results that pH of the solution has a stronger effect on the single-chain conformation and the self-assembly behavior of the peptides with larger blocks of similarly charged monomers. It has already been shown that intra-chain electrostatic interactions play an important role in the equilibrium conformation of block polyampholytes containing large blocks of similarly charged monomers (Baratlo and Fazli 2009, 2010).

References

Baratlo M, Fazli H (2009) Molecular dynamics simulation of semiflexible polyampholyte brushes–the effect of charged monomers sequence. Eur Phys J E 29:131–138. doi:10.1140/epje/i2009-10458-x

Baratlo M, Fazli H (2010) Brushes of flexible, semiflexible, and rodlike diblock polyampholytes: molecular dynamics simulation and scaling analysis. Phys Rev E 81:011801. doi:10.1103/PhysRevE.81.011801

Berendsen HJC, Postma JPM, van Gunsteren WF, Hermans J (1981) Interaction models for water in relation to protein hydration. Intermol Forces 14:331–342. doi:10.1007/978-94-015-7658-1_21

Berendsen HJC, Postma JPM, van Gunsteren WF, DiNola A, Haak JR (1984) Molecular dynamics with coupling to an external bath. J Chem Phys 81:3684–3690. doi:10.1063/1.448118

Carrell RW, Gooptut B (1998) Conformational changes and disease—serpins, prions and Alzheimer's. Curr Opin Struct Biol 8:799–809. doi:10.1016/S0959-440X(98)80101-2

Darden T, York D, Pedersen L (1993) Particle mesh Ewald: an *N*·log(*N*) method for Ewald sums in large systems. J Chem Phys 98:10089–10092. doi:10.1063/1.464397

Dubrynin AV, Colby RH, Rubinstein M (2004) Polyampholytes. J Polym Sci Part B Polym Phys 42:3513–3538. doi:10.1002/polb.20207

Emamyari S, Fazli H (2014) pH-dependent self-assembly of EAK16 peptides in the presence of a hydrophobic surface: coarse-grained molecular dynamics simulation. Soft Matter (to be published)

Essmann U, Perera L, Berkowitz ML, Darden T, Lee H, Pedersen LG (1995) A smooth particle mesh Ewald method. J Chem Phys 103:8577–8592. doi:10.1063/1.470117

Fernández-Carneado J, Kogan MJ, Pujals S, Giralt E (2004) Amphipathic peptides and drug delivery. Pept Sci 76:196–203. doi:10.1002/bip.10585

Ferreira ST, De Felice FG (2001) Protein dynamics, folding and misfolding: from basic physical chemistry to human conformational diseases. FEBS Lett 498:129–134. doi:10.1016/S0014-5793(01)02491-7

Fung SY, Keyes C, Duhamel J, Chen P (2003) Concentration effect on the aggregation of a self-assembling oligopeptide. Biophys J 85:537–548. doi:10.1016/S0006-3495(03)74498-1

Hess B, Bekker H, Berendsen HJC, Fraaije JGEM (1997) LINCS: a linear constraint solver for molecular simulations. J Comp Chem 18:1463–1472. doi:10.1002/(SICI)1096-987X(199709)18:12<1463::AID-JCC4>3.0.CO;2-H

Hess B, Kutzner C, van der Spoel D, Lindahl E (2008) GROMACS 4: algorithms for highly efficient, load-balanced, and scalable molecular simulation. J Chem Theory Comput 4:435–447. doi:10.1021/ct700301q

Holmes TC, de Lacalle S, Su X, Liu G, Rich A, Zhang S (2000) Extensive neurite outgrowth and active synapse formation on self-assembling peptide scaffolds. Proc Natl Acad Sci USA 97:6728–6733. doi:10.1073/pnas.97.12.6728

Hong Y, Legge RL, Zhang S, Chen P (2003) Effect of amino acid sequence and pH on nanofiber formation of self-assembling peptides EAK16-II and EAK16-IV. Biomacromolecules 4:1433–1442. doi:10.1021/bm0341374

Hong Y, Lau LS, Legge RL, Chen P (2004) Critical self-assembly concentration of an ionic-complementary peptide EAK16-I. J Adhesion 80:913–931. doi:10.1080/00218460490508616

Hong Y, Pritzker MD, Legge RL, Chen P (2005) Effect of NaCl and peptide concentration on the self-assembly of an ionic-complementary peptide EAK16-II. Colloids Surf B 46:152–161. doi:10.1016/j.colsurfb.2005.11.004

Houseman BT, Mrksich M (2002) Towards quantitative assays with peptide chips: a surface engineering approach. Trends Biotechnol 20:279–281. doi:10.1016/S0167-7799(02)01984-4

Humphrey W, Dalkeand A, Schulten K (1996) VMD: visual molecular dynamics. J Mol Graph 14:33–38. doi:10.1016/0263-7855(96)00018-5

HyperChem(TM), Hypercube, Inc., 1115 NW 4th Street, Gainesville, Florida 32601, USA

Jorgensen WL, Tirado-Rives J (1988) The OPLS potential functions for proteins. Energy minimizations for crystals of cyclic peptides and crambin. J Am Chem Soc 110:1657–1666. doi:10.1021/ja00214a001

Jun S, Hong Y, Imamura H, Ha B-Y, Bechhoefer J, Chen P (2004) Self-assembly of the ionic peptide EAK16: the effect of charge distributions on self-assembly. Biophys J 87:1249–1259. doi:10.1529/biophysj.103.038166

Kisiday J, Jin M, Kurz B, Hung H, Semino C, Zhang S, Grodzinsky AJ (2002) Self-assembling peptide hydrogel fosters chondrocyte extracellular matrix production and cell division: implications for cartilage tissue repair. Proc Natl Acad Sci USA 99:9996–10001. doi:10.1073/pnas.142309999

Lim HS, Han JT, Kwak D, Jin M, Cho K (2006) Photoreversibly switchable superhydrophobic surface with erasable and rewritable pattern. J Am Chem Soc 128:14458–14459. doi:10.1021/ja0655901

Luo Z, Zhao X, Zhang S (2008) Structural dynamic of a self-assembling peptide d-EAK16 made of only d-amino acids. PLoS ONE 3(5):e2364. doi:10.1371/journal.pone.0002364

Miyamoto S, Kollman PA (1992) Settle: an analytical version of the SHAKE and RATTLE algorithm for rigid water models. J Comp Chem 13:952–962. doi:10.1002/jcc.540130805

Sheng Y, Wang Y, Chen P (2010) Interaction of an ionic complementary peptide with a hydrophobic graphite surface. Protein Sci 19:1639–1648. doi:10.1002/pro.444

Soto C, Saborio GP (2001) Prions: disease propagation and disease therapy by conformational transmission. TRENDS Mol Med 7:109–114. doi:10.1016/S1471-4914(01)01931-1

van der Spoel D, Lindahl E, Hess B, Groenhof G, Mark AE, Berendsen HJC (2005a) GROMACS: fast, flexible, and free. J Comp Chem 26:1701–1718. doi:10.1002/jcc.20291

van der Spoel D, Lindahl E, Hess B, Kutzner C, van Buuren AR, Apol E, Meulenhoff PJ, Tieleman DP, Sijbers ALTM, Feenstra KA, van Drunen R, Berendsen HJC (2005b). Gromacs user manual version 4.0. www.gromacs.org

van Gunsteren WF, Berendsen HJC (1988) A Leap-frog algorithm for stochastic dynamics. Mol Sim 1:173–185. doi:10.1080/08927028808080941

Wang J, Tang F, Li F, Lin J, Zhang Y, Du L, Zhao X (2008a) The amphiphilic self-assembling peptide EAK16-I as a potential hydrophobic drug carrier. J Nanomater 2008:516286–516294. doi:10.1155/2008/516286

Wang X, Horii A, Zhang S (2008b) Designer functionalized self-assembling peptide nanofiber scaffolds for growth, migration, and tubulogenesis of human umbilical vein endothelial cells. Soft Matter 4:2388–2395. doi:10.1039/B807155A

Wei Y, Tong W, Wise C, Wei X, Armbrust K, Zimmt M (2006) Dipolar control of monolayer morphology: spontaneous SAM patterning. J Am Chem Soc 128:13362–13363. doi:10.1021/ja065338t

Whitesides GM, Boncheva M (2002) Beyond molecules: self-assembly of mesoscopic and macroscopic components. Proc Natl Acad Sci USA 99:4769–4774. doi:10.1073/pnas.082065899

Whitesides GM, Grzybowski B (2002) Self-assembly at all scales. Science 295:2418–2421. doi:10.1126/science.1070821

Whitesides GM, Mathias JP, Seto C (1991) Molecular self-assembly and nanochemistry: a chemical strategy for the synthesis of nanostructures. Science 254:1312–1319. doi:10.1126/science.1962191

Wouters D, Schubert US (2004) Nanolithography and nanochemistry: probe-related patterning techniques and chemical modification for nanometer-sized devices. Angew Chem Int Ed 43:2480–2495. doi:10.1002/anie.200300609

Yan Z, Wang J, Wang W (2008) Folding and dimerization of the ionic peptide EAK16-IV. Proteins 72:150–162. doi:10.1002/prot.21903

Yang H, Fung S-Yu, Pritzker M, Chen P (2007a) Surface-assisted assembly of an ionic-complementary peptide: controllable growth of nanofibers. J Am Chem Soc 129(12200):12210. doi:10.1021/ja073168u

Yang H, Fung S-Yu, Pritzker M, Chen P (2007b) Modification of hydrophilic and hydrophobic surfaces using an ionic-complementary peptide. PLoS ONE 2:e1325. doi:10.1371/journal.pone.0001325

Zerovnik E (2002) Amyloid-fibril formation: proposed mechanisms and relevance to conformational disease. Eur J Biochem 269:3362–3371. doi:10.1046/j.1432-1033.2002.03024.x

Zhang S (2003) Fabrication of novel biomaterials through molecular self-assembly. Nat Biotechnol 21:1171–1178. doi:10.1038/nbt874

Zhang S, Lockshin C, Herbert A, Winter E, Rich A (1992) Zuotin, a putative Z-DNA binding protein in Saccharomyces cerevisiae. EMBO J 11:3787–3796

Zhang S, Holmes T, Lockshin C, Rich A (1993) Spontaneous assembly of a self-complementary oligopeptide to form a stable macroscopic membrane. Proc Natl Acad Sci USA 90:3334–3338. doi:10.1073/pnas.90.8.3334

Zhang S, Holmes TC, Michael DiPersio C, Hynes RO, Su X, Rich A (1995) Self-complementary oligopeptide matrices support mammalian cell attachment. Biomaterials 16:1385–1393. doi:10.1016/0142-9612(95)96874-Y

Zhang S, Yan L, Altman M, Lässle M, Nugent H, Frankel F, Lauffenburger DA, Whitesides GM, Rich A (1999) Biological surface engineering: a simple system for cell pattern formation. Biomaterials 20:1213–1220. doi:10.1016/S0142-9612(99)00014-9

Zhang S, Marini DM, Hwang W, Santoso S (2002) Design of nanostructured biological materials through self-assembly of peptides and proteins. Curr Opin Chem Biol 6:865–871. doi:10.1016/s1367-5931(02)00391-5